J Physiol 593.8 (2015) pp 1809–1827

The Journal of Physiology

TECHNIQUES FOR PHYSIOLOGY

The use of murine-derived fundic organoids in studies of gastric physiology

Michael A. Schumacher[1], Eitaro Aihara[1], Rui Feng[1], Amy Engevik[1], Noah F. Shroyer[2], Karen M. Ottemann[3], Roger T. Worrell[1], Marshall H. Montrose[1], Ramesh A. Shivdasani[4] and Yana Zavros[1]

[1]*Department of Molecular and Cellular Physiology, University of Cincinnati College of Medicine, Cincinnati, OH, USA*
[2]*Department of Medicine Section of Gastroenterology and Hepatology, Baylor College of Medicine, Houston, TX, USA*
[3]*Department of Microbiology and Environmental Toxicology, University of California at Santa Cruz, Santa Cruz, CA, USA*
[4]*Department of Medical Oncology, Dana-Farber Cancer Institute, and Department of Medicine, Harvard Medical School, Boston, MA, USA*

Key points

- An *in vitro* approach to study gastric development is primary mouse-derived epithelium cultured as three-dimensional spheroids known as organoids.
- We have devised two unique gastric fundic-derived organoid cultures: model 1 for the expansion of gastric fundic stem cells, and model 2 for the maintenance of mature cell lineages.
- Organoids maintained in co-culture with immortalized stomach mesenchymal cells express robust numbers of surface pit, mucous neck, chief, endocrine and parietal cells.
- Histamine induced a significant decrease in intraluminal pH that was reversed by omeprazole in fundic organoids and indicated functional activity and regulation of parietal cells. Localized photodamage resulted in rapid cell exfoliation coincident with migration of neighbouring cells to the damaged area, sustaining epithelial continuity.
- We report the use of these models for studies of epithelial cell biology and cell damage and repair.

Abstract Studies of gastric function and disease have been limited by the lack of extended primary cultures of the epithelium. An *in vitro* approach to study gastric development is primary mouse-derived antral epithelium cultured as three-dimensional spheroids known as organoids. There have been no reports on the use of organoids for gastric function. We have devised two unique gastric fundic-derived organoid cultures: model 1 for the expansion of gastric fundic stem cells, and model 2 for the maintenance of mature cell lineages. Both models were generated from single glands dissociated from whole fundic tissue and grown in basement membrane matrix (Matrigel) and organoid growth medium. Model 1 enriches for a stem cell-like niche via simple passage of the organoids. Maintained in Matrigel and growth medium, proliferating organoids expressed high levels of stem cell markers CD44 and Lgr5. Model 2 is a system of gastric organoids co-cultured with immortalized stomach mesenchymal cells (ISMCs). Organoids maintained in co-culture with ISMCs express robust numbers of surface pit, mucous neck, chief, endocrine and parietal cells. Histamine induced a significant decrease in intraluminal pH that was reversed by omeprazole in fundic organoids and indicated functional activity and regulation of parietal cells. Localized photodamage resulted in rapid cell exfoliation coincident with migration of neighbouring cells to the damaged area, sustaining epithelial continuity. Thus, we report the use of these models for studies of epithelial cell biology and cell damage and repair.

M. A. Schumacher, E. Aihara and R. Feng are contributed equally.

DOI: 10.1113/jphysiol.2014.283028

(Received 22 August 2014; accepted after revision 16 January 2015; first published online 19 February 2015)
Corresponding author Y. Zavros: University of Cincinnati College of Medicine, Department of Molecular and Cellular Physiology, 231 Albert B. Sabin Way, Room 4255 MSB, Cincinnati, OH 45267-0576, USA. Email: yana.zavros@uc.edu

Abbreviations DMEM, Dulbecco's modified Eagle medium; DPBS, Dulbecco's phosphate-buffered saline; EdU, 5-ethynyl-2′-deoxyuridine; ISMCs, immortalized stomach mesenchymal cells; Lgr5, leucine-rich repeat-containing G protein-coupled receptor 5; SPEM, spasmolytic polypeptide expressing metaplasia; UEAI, *Ulex europaeus* I.

Introduction

Studies of gastric function and disease have been limited to the use of *in vitro* immortalized or gastric cancer cell lines or *in vivo* animal models. An emerging *in vitro* approach that may be uniquely beneficial to study gastric physiology and disease is the primary mouse-derived epithelium cultured as three-dimensional (3D) spheroids known as organoids. Despite the extensive use of these culture systems for the study of stem cell biology and gastrointestinal development (Jaks *et al.* 2008; Barker *et al.* 2010; Stange *et al.* 2013), the degree to which these cultures reflect the function of native tissue has not been reported. Therefore, the capacity for use in functional studies of physiological research has been limited. Our study represents a technical advance in the field of physiology. The fundic organoid culture model represents our ability to replicate the gastrointestinal environment *in vitro*, and therefore in time may supersede some of the existing cell line- and tissue-based systems to study the mechanism of gastric acid secretion, *Helicobacter* adherence and pathogenesis, hormonal signalling and tissue repair.

The gastric epithelium is a self-renewing tissue that is anatomically divided into two major functional regions: (1) the fundus (or corpus), comprising the parietal, chief, surface mucous pit and mucous neck cells; and (2) the antrum composed of predominantly mucus-producing cells. Endocrine cells are found in both the fundus and the antrum (Mills & Shivdasani, 2011). Based on studies demonstrating that the leucine-rich repeat-containing G protein-coupled receptor 5 (Lgr5) may be used as a marker of stem cells in the gastric antrum, it is now possible to establish long-term primary gastric cultures (Jaks *et al.* 2008; Barker *et al.* 2010). However, such a system has not been established for the fundus (or corpus) of the stomach where Lgr5-positive cells are not expressed in the adult (Barker *et al.* 2010). The corpus epithelium is organized into gastric units that contain the cell lineages in four distinct zones that are the surface pit, isthmus, neck and base regions (Mills & Shivdasani, 2011). Extensive studies by Karam & Leblond (1993) combined tritiated thymidine labelling with electron microscopy to examine the pathways of cell renewal of the gastric epithelium. Based on these studies, the isthmus region of the gastric gland is generally accepted as the zone that contains undifferentiated progenitor or 'stem' cells (Karam & Leblond, 1993). Stem cells anchored in the isthmus region are responsible for the production of parietal cells (Karam & Leblond, 1993), and distinct from the recently identified stem cells marked by *Troy* that are expressed at the corpus gland base in a subset of differentiated chief cells (Stange *et al.* 2013). Although Stange *et al.* (2013) demonstrate that *Troy*-positive chief cells may be used to generate long-lived gastric organoids, *in vitro* these cultures are differentiated toward the mucus-producing cell lineages of the neck and pit regions. Our study advances these findings by not only generating an organoid culture that maintains all the major cell lineages of the fundus, but also documents the functional capacity of this system.

We have devised two unique gastric fundic-derived organoid cultures: model 1 for the expansion of gastric fundic stem cells that consist of approximately 90% CD44/Lgr5+ stem cells, and model 2 for the maintenance of mature cell lineages that include surface mucous pit, mucous neck, chief, endocrine, parietal and CD44/Lgr5+ cells (Fig. 1). Model 1 enriches for a stem cell-like niche via simple passage of the organoids. Maintained in *Matrigel* and gastric organoid growth medium, organoids were proliferative and expressed high levels of stem cell markers CD44 and Lgr5. Model 2 is a system of gastric organoids co-cultured with immortalized stomach mesenchymal cells (ISMCs) and express robust numbers of surface pit, mucous neck, chief, endocrine and parietal cells. Using these models, we demonstrate assays of epithelial barrier function, cellular restitution and pH response. The fundic organoid culture model represents a significant advance in our ability to replicate the gastrointestinal environment *in vitro*.

Methods

Fundic organoid generation and culture

C57BL/6 or Yellow cameleon 3.0 (YC3.0) transgenic (Nyqvist *et al.* 2005; Aihara *et al.* 2013) mice (aged 8–10 weeks) were used for fundic and antral gastric organoid cultures. Methods were approved by our University Committee on Use and Care of Animals and are consistent with recommendations of the Panel on Euthanasia of the American Veterinary Medical Association. Animals were killed via carbon dioxide inhalation followed by cervical dislocation prior to removal of stomach. Animals were killed and stomachs

removed, opened along the greater curvature and washed in ice-cold Dulbecco's phosphate-buffered saline (DPBS). Serosal muscle was removed from fundic or antral tissue under a dissecting microscope using micro-dissecting scissors and fine forceps (examples of preparation are shown in Fig. 2). There was a clear delineation and separation of collected fundic and antral tissue as shown by the dotted lines in Fig. 2. Tissue was cut into <5 mm^2 pieces and incubated rocking at 4°C for 2 h in DPBS without calcium and magnesium (DPBS w/o Ca^{2+}/Mg^{2+}) +5 mM EDTA (Sigma-Aldrich, St Louis, MO, USA). Tissue was removed and placed into 5 ml dissociation buffer (43.4 mM sucrose, 54.9 mM D-sorbitol (Sigma-Aldrich), in DPBS), and shaken vigorously for 2 min by hand to dissociate individual glands from tissue, followed by mechanical dissociation using a 1000 μl pipette to obtain the desired gland concentration. Medium containing dissociated glands was centrifuged at 150 *g* for 5 min, and the pellet re-suspended in Matrigel (BD Biosciences, Franklin Lakes, NJ, USA). Suspended glands in Matrigel were added to 12-well culture plates (50 μl Matrigel per well) or two-well dishes (for microinjection and imaging). After Matrigel polymerization at 37°C, gastric organoid growth medium (Advanced DMEM/F12 (12634-010; Life Technologies, Carlsbad, CA, USA) containing Wnt conditioned medium (50%), R-spondin conditioned medium (10%), [Leu15]-Gastrin I (10 nM: Sigma-Aldrich), *N*-acetylcysteine (1 mM: Sigma-Aldrich), FGF10 (100 ng ml^{-1}: Pepro Tech, London, UK), EGF10 (epidermal growth factor 10, 50 ng ml: Pepro Tech), Noggin (100 ng ml^{-1}: Pepro Tech) and Y-27632 (initial 4 days only, 10 nM, Sigma-Aldrich)) was added to wells and replaced every 4 days.

To test for optimal growth and efficiency, a panel of growth conditions were assayed by removing each individual growth factor successively. Removal of EGF10, Noggin, [Leu15]-Gastrin I, Wnt conditioned medium and R-spondin conditioned medium resulted in stunted

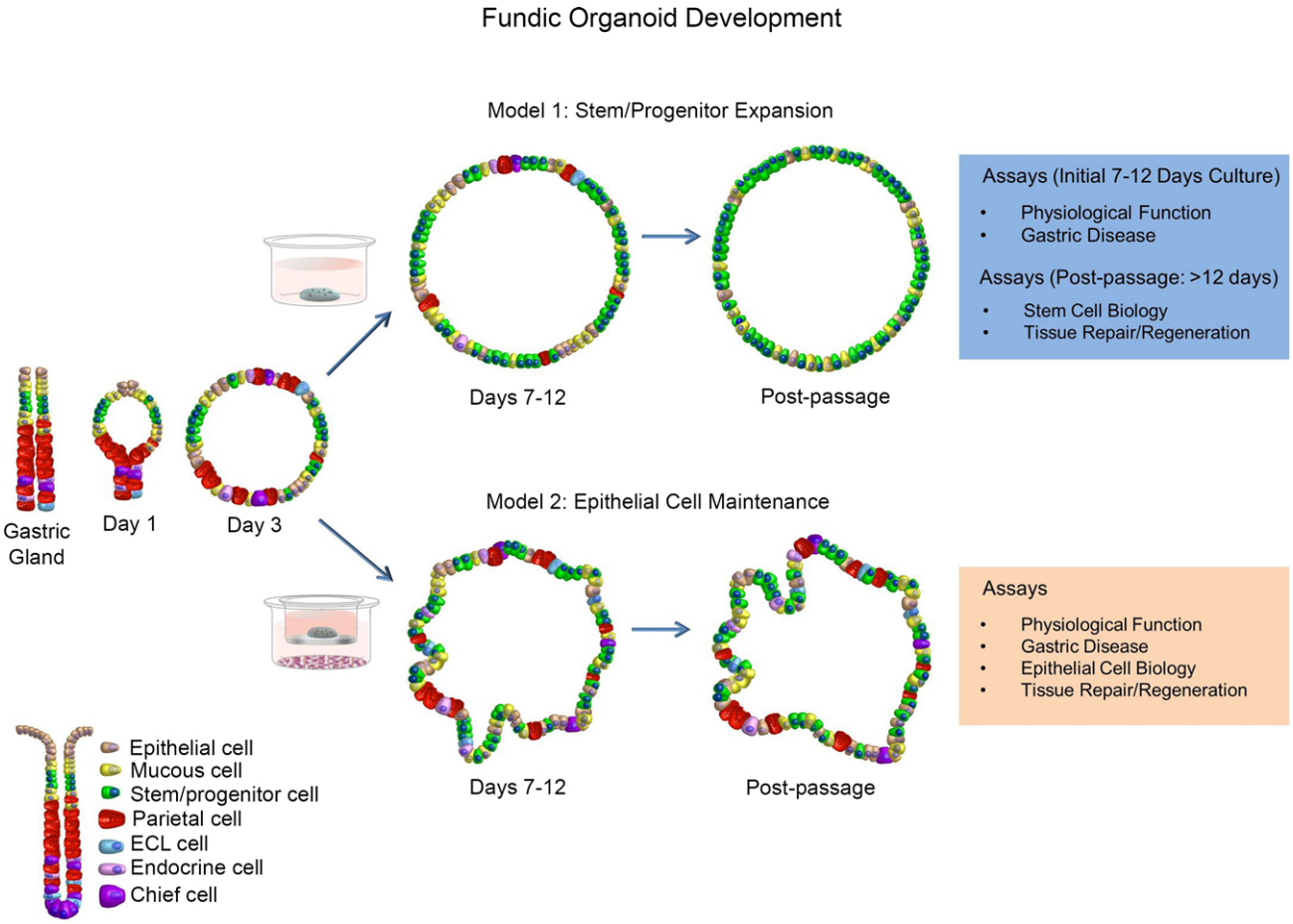

Figure 1. Schematic diagram showing the development of two organoid culture systems that may be used for studies of gastric physiological function and disease
Model 1 represents a system whereby stem/progenitor cells are expanded for studies in stem cell biology and tissue repair/regeneration. Model 2 represents a culture system of maintained epithelial cells for studies of physiological function, gastric disease and epithelial cell biology.

growth and inability for organoids to survive past day 7. Use of complete medium resulted in the highest growth efficiency (Fig. 3*A*, *B*) and size (Fig. 3*A*, *C*) and demonstrated that EGF10, Noggin, [Leu15]-Gastrin I, and Wnt and R-spondin conditioned media were necessary for growth of organoids. Interestingly removal of R-spondin conditioned medium led to a failure of organoids to grow (Fig. 3). While the removal of Wnt conditioned medium did not inhibit the initial formation of the organoids, reduced speed of growth and failure to thrive past day 7 was observed (Fig. 3).

Generating Wnt and R-spondin conditioned media

L cells were received as a gift from Dr Hans Clevers (Hubrecht Institute for Developmental Biology and Stem Cell Research, Netherlands). Cells were grown in Dulbecco's modified Eagle medium (DMEM) supplemented with 10% fetal bovine serum (FBS) and 1% penicillin/streptomycin for 7 days, then medium was collected and filtered through 0.22 μm filter B (Barker *et al.* 2010). A modified HEK-293T R-spondin secreting cell line was donated by Dr Jeff Whitsett (Section of Neonatology, Perinatal and Pulmonary Biology, Cincinnati Children's Hospital Medical Centre and The University of Cincinnati College of Medicine, Cincinnati, USA). Cells were grown in DMEM supplemented with 10% FBS and 1% penicillin/streptomycin. Once cells attached to the plate, medium was changed to OPTIMEM (Invitrogen, Carlsbad, CA, USA) supplemented with 1% penicillin/streptomycin. Seven days later, medium was collected and filtered through a 0.22 μm filter (Bell *et al.* 2008).

TOPflash assay

Both Wnt and R-spondin conditioned media activities were assayed by TOPFlash. TOPFlash vector was kindly donated by Dr H. Clevers. HEK-293T cells were plated on 24-well tissue culture plates at 30 000 cells per well and simultaneously transfected with luciferase reporter of beta-catenin-mediated transcriptional activation (TCF/LEF biding sites), TOPflash vector, or its control luciferase reporter, FOPflash (mutant of TCF/LEF binding sites). TOPflash and FOPflash reporter constructs were kindly provided by Dr H. Clevers.

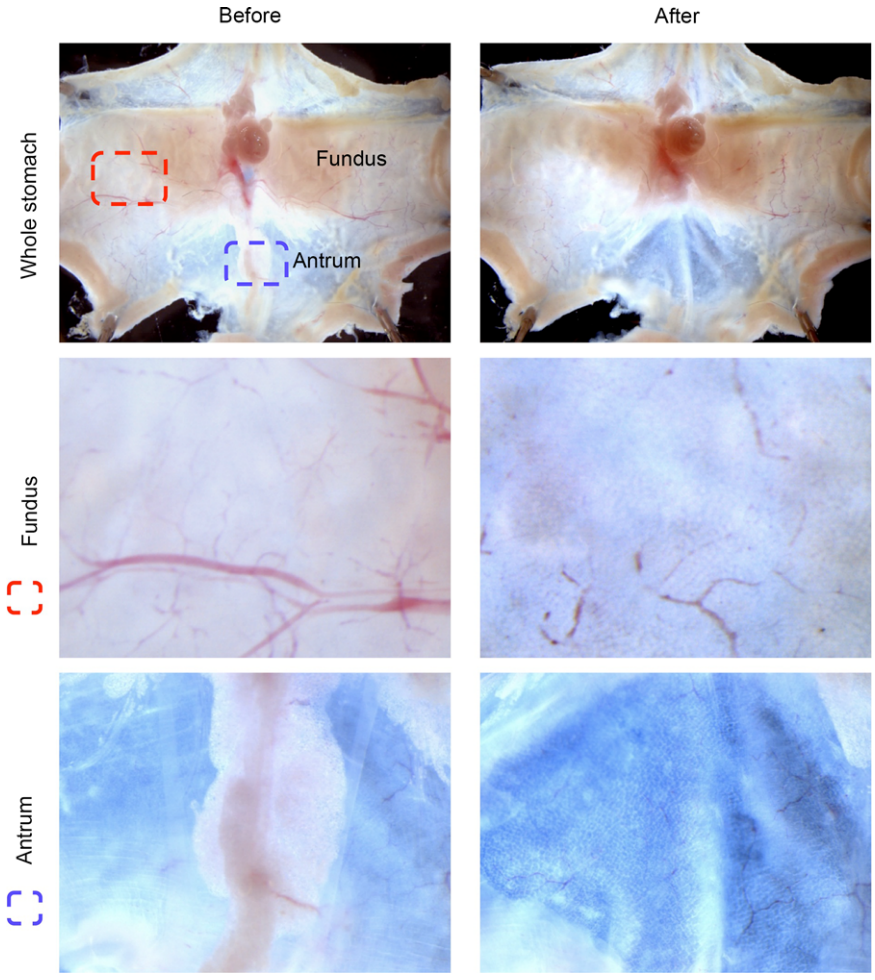

Figure 2. Fundic and antral dissection
Stomachs were opened along the greater curvature, and washed in ice-cold DPBS. Stomachs were pinned and muscle was stripped using dissecting scissors and a microscope. Images before and after muscle stripping are shown for fundus and antrum. Tissue collected for gland isolation is shown by dotted lines, demonstrating collection of distinct regions for fundus and antrum for organoid preparation.

Transfections were performed using polytheylenimine, linear MW-25000 (Polysciences, Warrington, PA, USA) transfection reagent. A pRL renilla luciferase control reporter vector (Promega, Madison, WI, USA) served as a control for transfection efficiency. HEK-293T cells were transfected for 16 h in DMEM supplemented with 10% FBS, and 1% penicillin/streptomycin. Afterwards, HEK-293 T cells were treated with Wnt or R-spondin conditioned media for 24 h. Cells were lysed, and cell lysates were assayed for firefly luciferase and renilla luciferase activity on a luminometer using the Dual-Luciferase reporter assay system following the manufacturer's protocols (Promega). TOPflash and FOPflash luciferase activities were normalized to renilla luciferase activity.

Stem cell/progenitor expansion (model 1)

To enrich for the stem cells or progenitors, gastric organoids were passaged every 12 days. Organoids were

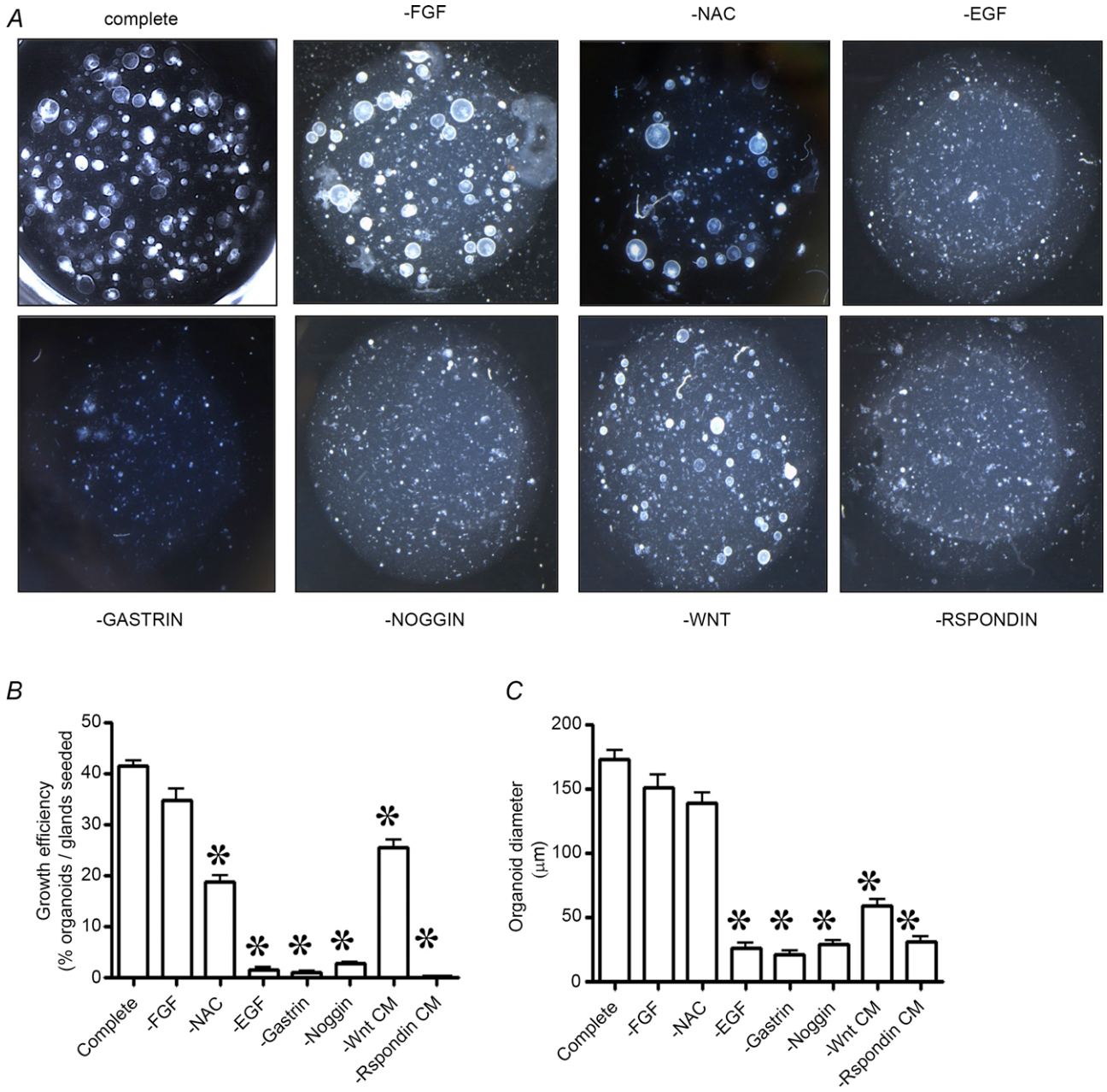

Figure 3. Determination of optimal growth conditions for fundic gastric organoids
A, the requirement for growth factors is demonstrated in representative images at day 7 of culture. *B*, fundic organoid growth efficiency (percentage organoids per glands seeded). *C*, size (at day 7) was assayed in primary cultures by removing each individual growth factor from growth medium. $^*P < 0.05$ compared to complete.

removed from Matrigel using ice-cold DPBS, broken up by passing through a 26 G needle and fractions were centrifuged at 150 *g* for 5 min. The pellet was re-suspended in Matrigel followed by addition of growth medium as described above.

Maintenance of epithelial cell lineages (model 2)

To maintain a mature phenotype we implemented a Transwell system whereby gastric organoids were co-cultured with ISMCs (Feng *et al.* 2014), cells previously shown to induce embryonic endoderm to differentiate to a gastric phenotype (Kim *et al.* 2005). The ISMCs were generated by immortalizing embryonic day (E) 13.5 wild-type CD1 mouse stomach mesenchymal cell cultures with a dominant-negative Tp53-encoding retrovirus and expanding cells for multiple passages beyond the death of uninfected cells (Shaulian *et al.* 1992). Organoids were grown in Matrigel as described above on the top side of a polyester Transwell insert (0.4 μm pore size, Dow Corning, Midland, MI, USA) with gastric organoid medium seeded on the bottom and top of wells. At day 4, 1.2×10^4 ISMCs were seeded on the bottom of a 12-well plate and organoid-containing Transwell inserts were transferred to the wells. Medium and ISMCs were replaced every other day. At day 10–12 organoids were harvested for use in subsequent experiments.

Flow cytometry

Fundic gastric organoids grown with or without ISMCs were collected at day 4, 7 and 12 using ice cold DPBS. Single cells were obtained by treating organoids with dispase II (1 mg ml^{-1}, Roche, Indianapolis, IN, USA) for 20–30 min while shaking at 37 °C. Cells were labelled with cell surface markers CD44 and Lgr5 using FITC rat anti-mouse CD44 (1:50, 561859; BD Pharmingen) and anti-human Lgr5 PE conjugated (1:50, TA400001; OriGene, Rockville, MD, USA) antibodies. Cells were then fixed and permeabilized according to the manufacturer's protocol (Invitrogen Fix & Perm kit, GAS004) and then co-stained using rabbit anti-DCAMKL1 antibody (1:33, ab37994; Abcam, Cambridge, MA, USA) followed by a 1:100 diluation of anti-rabbit IgG APC conjugated secondary antibody (ab72567; Abcam). In a separate tube of fixed and permeabilized cells, samples were incubated with lectin FITC labelled *Ulex europaeus* (UEAI, 1:100 dilution, Sigma-Aldrich), lectin *Griffonia simplicifolia* Alexa Fluor 647 (GSII, 1:100 dilution, Molecular Probes) and then rabbit anti-intrinsic factor (1:100 dilution, ab1322; Abcam) followed by a 1:100 dilution of anti-rabbit IgG PE secondary antibody (ab7070; Abcam). In a third tube of fixed and permeabilized cells, cells were immunostained using a 1:100 dilution of anti-chromagranin A antibody (ab15160; Abcam) followed by a 1:100 dilution of anti-rabbit IgG PE conjugated secondary antibody. Finally, in a fourth tube of fixed and permeabilized cells, cells were labelled using a 1:100 dilution of anti-human gastrin (Novacastra, Buffalo Grove, IL, USA) and anti-HK-ATPase (MA3-923; Affinity Bioreagents, Golden, CO, USA) antibodies followed by secondary antibodies anti-rabbit IgG APC conjugated and anti-mouse IgG FITC conjugated (ab6785; Abcam) at a 1:100 dilution. All antibody incubations were performed at room temperature for 20 min. Cells were analysed using the FACSCalibur flow cytometer (BD Biosciences) and FloJo software (Tree Star, Ashland, OR, USA).

Quantitative RT-PCR

Total RNA was isolated from gastric glands or cultured gastric organoids. cDNA was synthesized (High Capacity cDNA Reverse Transcription Kit; Applied Biosystems, Foster City, CA, USA) and analysed by real-time PCR (TaqMan, Applied Biosystems) using pre-validated TaqMan primers: Pepsinogen C (Mm01278038_m1), Somatostatin (Mm00436671_m1), H^+,K^+-ATPase (Mm01176574), Gastrin (Mm00439059), Muc5AC (Mm01276711), Muc6 (Mm00725185), CD44 (Mm01277163_m1), DCLK1 (Mm00444950_m1), *Troy* (Mm00443506_m1), Cdx1 (Mm00438172_m1), Cdx2 (Mm01212280_m1), TFF2 (Mm00447491_m1), TFF3 (Mm00495590_m1), HE4 (Mm00509434_m1), MUC2 (Mm01276696_m1) and HPRT (Mm00446968_m1). PCR amplifications were performed in 20 μl containing 20× TaqMan Expression Assay primers, 2× TaqMan Universal Master Mix (TaqMan Gene Expression Systems; Applied Biosystems) and cDNA. PCR amplification (StepOne Real-Time PCR System, Applied Biosystems) used the following conditions: 50°C for 2 min, 95°C for 10 min, 95°C for 15 s (denature) and 60°C for 1 min (anneal/extend) for 40 cycles. LGR5 expression was quantified using specific primers for LGR5: forward, 5-CCTACTCGAAGACTTACCCAGT-3; and reverse, 5-GCATTGGGGTGAATGATAGC-3 using the SYBR Green PCR Master Mix and protocol (Applied Biosystems). Fold change was calculated as $(C_t – C_{t\,high}) = n_{target}$, $2^{ntarget}/2^{nHPRT}$ = fold change where C_t = threshold cycle. The results were expressed as average fold change in gene expression relative to the uninfected or control group, and HPRT was used as an internal control. Data were calculated according to Livak & Schmittgen (2001).

Immunofluorescence staining

Organoids were removed from Matrigel using ice-cold DPBS, and fixed in 4% paraformaldehyde for 30 min, followed by Histogel (Thermo Scientific, Waltham,

MA, USA) and paraffin embedding. Sections of 5 μm were cut for immunofluorescence staining. Sections for immunofluorescence were blocked with 5% BSA before incubation with antibodies for gastric H^+/K^+-ATPase (1:1000, MA3;923; Affinity Bioreagents) and Rhodamine-conjugated UEAI (1:5000, RL-1062; Vector Labs, Philadelphia, PA, USA) overnight at 4°C. Sections were then incubated for 1 h at room temperature with secondary antibody Alexa Fluor 633 (1:1000; Invitrogen). Sections were imaged using a Zeiss LSM510 microscope.

Whole mount staining was performed on organoids 7 days of age for E-cadherin, H^+/K^+-ATPase, Intrinsic Factor and Chromogranin A. Organoids suspended in Matrigel were fixed with 4% paraformaldehyde for 30 min at room temperature, followed by tissue permeabilization with 0.5% Triton X-100 in PBS for 20 min, then blocking in 20% serum specific to the animal that the secondary antibody was raised in. E-cadherin (1:1000, sc59778; Santa Cruz Biotechnology, Santa Cruz, CA, USA), H^+/K^+-ATPase (1:1000, MA3-923; Affinity Bioreagents), Intrinsic Factor (1:1000, ab91322; Abcam) or Chromogranin A (1:500, ab15160; Abcam) were incubated overnight at 4°C. Next, organoids were incubated with Alexa Flour 488 or 633 (1:1000; Invitrogen) for 1 h at room temperature, followed by nuclear stain (Hoechst 33342, 10 μg ml^{-1}; Invitrogen) for 20 min. Whole mount sections were obtained via Z-stack reconstruction using the Zeiss LSM710.

EdU labelling

To identify the number of proliferating cells, gastric organoids were incubated in 5 μM 5-ethynyl-2′-deoxyuridine (EdU) (C10639; Invitrogen) in DMEM for 1 h at 37°C. Organoids were then fixed for 15 min with 3.7% formaldehyde in PBS followed by permeabilization using 0.5% Triton X-100 in PBS for 20 min at room temperature. The 'Click-iT' reaction cocktail (C10639; Invitrogen) was added to the cells according to the manufacturer's instructions and incubated for 30 min at room temperature, followed by two washes in PBS. Organoids were then incubated with DNA dye Hoechst 33342 (Invitrogen) at a dilution of 1:1000 in PBS for 30 min. Z-stack series of confocal images were taken using a Zeiss LSM710 LIVE Duo Confocal Microscope and analysed using IMARIS imaging software. Total cell number and EdU-labelled nuclei were counted and expressed as the ratio of EdU-positive cells versus total cells.

Confocal time lapse imaging microscopy

Gastric organoids were grown on chambered coverglass (Thermo Scientific) or removable Transwell inserts for live imaging. Experiments were performed with coverglass in organoid culture medium under 5% CO_2 and 37°C conditions (incubation chamber, PeCon, Erbach, Germany). The chamber was placed on an inverted confocal microscope (Zeiss LSM 710), and the growth of gastric organoids was monitored using a Zeiss EC plan-Neofluar 10× objective. Transmitted light images were collected at 30 min intervals.

Luminal pH of gastric organoids was measured using the ratiometric pH sensitive dye, 5-(and-6)-carboxy SNARF-1F or -5F (5 mM stock: excitation 514 nm, emission 550–620 and 620–700 nm; Invitrogen). Dye was microinjected (23 nl) and monitored using the Plan-Apochromat 20× objective. Histamine (100 μM; Sigma-Aldrich) or omeprazole (100 μM; Sigma-Aldrich) was added to the medium. Based on changes in pH and immunofluorescence staining of the H^+,K^+-ATPase, approximately 80% of fundic organoids were classified as highly responsive to treatment. Images were analysed using MetaMorph software (Molecular Devices, Downingtown, PA, USA). Background corrected 550–620/620–700 nm ratio values were converted to pH using a standard curve as described previously (Chu & Montrose, 1995).

Transmission electron microscopy

Organoids were fixed in 2% glutaraldehyde plus 2% paraformaldehyde in 0.1 M sodium cacodylate buffer (pH 7.4) overnight at 4°C. Organoids were then washed using 0.1 M sodium cacodylate buffer followed by a 1 h incubation using 4% osmium tetroxide, washed and then dehydrated using 25–100% ethanol (series of dilutions), embedded using propylene oxide/LX112. Blocks were sectioned (150 nm) and stained with 2% uranyl acetate followed by lead citrate. Tissue was visualized using a Hitachi transmission electron microscope equipped with an AMT Image Capture Engine version 5.42.366 and MicroFIRE (Optronics, Milton Keynes, UK) camera.

Acridine Orange experiments

Organoids were incubated with Acridine Orange (1 μM) for 15 min at 37°C/5% CO_2. Fluorescence of acridine orange was excited at 458 or 488 nm and images were collected in a time series at 600–650 or 500–550 nm, respectively. At each time point, a set of ten x–y plane images were taken at 6 μm focus intervals. Histamine (final concentration 100 μM) was applied to the medium.

Images were analysed by MetaMorph software (ver.6.3; Molecular Devices). The background-corrected F458/F488 fluorescence ratio image was calculated and normalized to a value of 1 in the histamine pretreatment baseline. The 3D images were created by Imaris software (ver.7.7; Bitplane, South Windsor, CT, USA).

Induction of laser-induced microlesion

Organoids in the PeCon chamber (5% CO_2, 37°C) were placed on the stage of an inverted confocal/two-photon microscope (Zeiss LSM 510 NLO) and imaged with a C-Achroplan NIR 40× objective. The organoid was pre-incubated with nuclear stain, Hoechst (10 μg ml^{-1}; Invitrogen), for 30 min while Lucifer yellow (50 μM; Invitrogen) was applied before the experiment. Confocal imaging recorded organoid structure (confocal reflectance 730 nm), Hoechst (excitation: 730 nm, emission: 435–485 nm), YFP (excitation: 514 nm, emission: 535–585 nm) or Lucifer yellow (excitation: 458 nm, emission: 500–550 nm). The method of causing microscopic photodamage in the tissue with a two-photon laser has been described previously (Xue *et al.* 2011). Briefly, after collecting a set of control images using minimal Ti–Sa (730 nm) laser power (<50 mW), a small rectangular region (<10 μm^2) of cells was repetitively scanned (700–1000 mW average laser power), for 150 iterations.

Statistical analyses

The significance of the results was tested by Student's *t* test using commercially available software (GraphPad Prism; GraphPad Software, San Diego, CA, USA). $P < 0.05$ was considered significant.

Results

Fundic gastric organoids enriched for stem cells

Figure 4 demonstrates our ability to maintain a long-term culture system for the fundic region of the mouse stomach. Fundic and antral gastric glands formed cyst-like structures visible within 3 days of culture (Fig. 4*A*). We determined the gene expression of gastric-specific cell lineage markers prior to the first passage. Both fundic and antral organoids expressed mRNA for mucin 5AC (surface mucous pit cells), mucin 6 (mucous neck cells), pepsinogen C (zymogen/chief cells) and somatostatin (D cells) as detected by quantitative (q)RT-PCR (Fig. 4*B*). In contrast, the expression of gastrin (G cells) was specific to antral organoids, whereas H^+,K^+-ATPase (parietal cells) was specific to fundic organoids (Fig. 4*B*). Time-lapse imaging of organoid formation over the initial 72 h showed proliferating cells of fundic gastric glands localized to a mid-gland region (Supporting Information, Video S1) as opposed to the base on antral glands (Video S2). Subsequently, proliferative regions of both antral and fundic glands expanded into epithelial spheroids.

Epithelial polarity was confirmed by apical membrane staining of *Ulex europaeus* I (UEAI) lectin on surface mucous pit cells (Fig. 4*C*) and basolateral membrane staining for E-cadherin (Fig. 4*C*). Moreover, luminal retention of micro-injected Lucifer yellow over 24 h confirmed the low transepithelial permeability of fundic organoids (Fig. 5*B–E*).

Prior to the first passage of the organoids, we confirmed cell-specific expression of parietal, chief and endocrine cell markers by immunostaining (Fig. 4*D*). To quantify the cellular composition we performed flow cytometric analysis of major gastric cell lineages using fundic organoids cultured for 4, 7 and 12 days. With culture the percentage of parietal, endocrine, chief and surface pit cells declined, but a population of cells co-expressing stem cell markers CD44 (Khurana *et al.* 2013) and Lgr5 (Barker *et al.* 2010) were enriched (Figs 4*E*, *F* and 5*F–K*). These data were confirmed by qRT-PCR, demonstrating a decrease in cell lineage markers (Fig. 4*G*) that correlated with an increase in stem cell markers (Fig. 4*H*). While cells expressing stem cell markers CD44 and Lgr5 expanded with passaging, *Troy* expression declined (Fig. 4*G*). We have cultured fundic gastric organoids for over 90 days (Fig. 5*A*). Therefore, our ability to sustain the fundic organoids in culture for several passages with an expansion in a cellular composition of cells expressing stem cell markers CD44 and Lgr5 suggests enrichment for a stem cell-like niche.

Maintenance of mature cell lineages within fundic gastric organoids

We next sought to develop a protocol to maintain the differentiated phenotype within the fundic gastric organoids. We adopted an approach used by investigators to drive embryonic gastric epithelial differentiation (Kim *et al.* 2005) using mouse-derived ISMCs in co-culture (Fig. 6*A*). By 3 days in co-culture the organoids displayed glandular structures and budding of the epithelium (Fig. 6*A*). Immunofluorescence staining of the H^+,K^+-ATPase-expressing parietal cells was elevated in organoids co-cultured with ISMCs (Fig. 6*B*) that were then quantified using flow cytometry. Flow cytometric analysis revealed that co-culture induced or maintained expression of major cell lineages (Figs 5*F–K* and 6*C*). In addition, there were significantly lower numbers of CD44/Lgr5-positive cells associated with model 2 in comparison with model 1 that may be a reflection of decreased stem cell proliferation in a system of sustained mature epithelial cells (Fig. 6*D*). We concluded that with ISMC co-culture an epithelium expressing mature tissue markers is maintained.

To determine the proliferative capacity of the cells within models 1 and 2, cultures were immunostained for EdU and proliferating cells werequantified (Fig. 6*E*, *F*). While there was maintenance of proliferating cells in the co-culture model 2 system, there was a significant decrease in the number of proliferating cells in

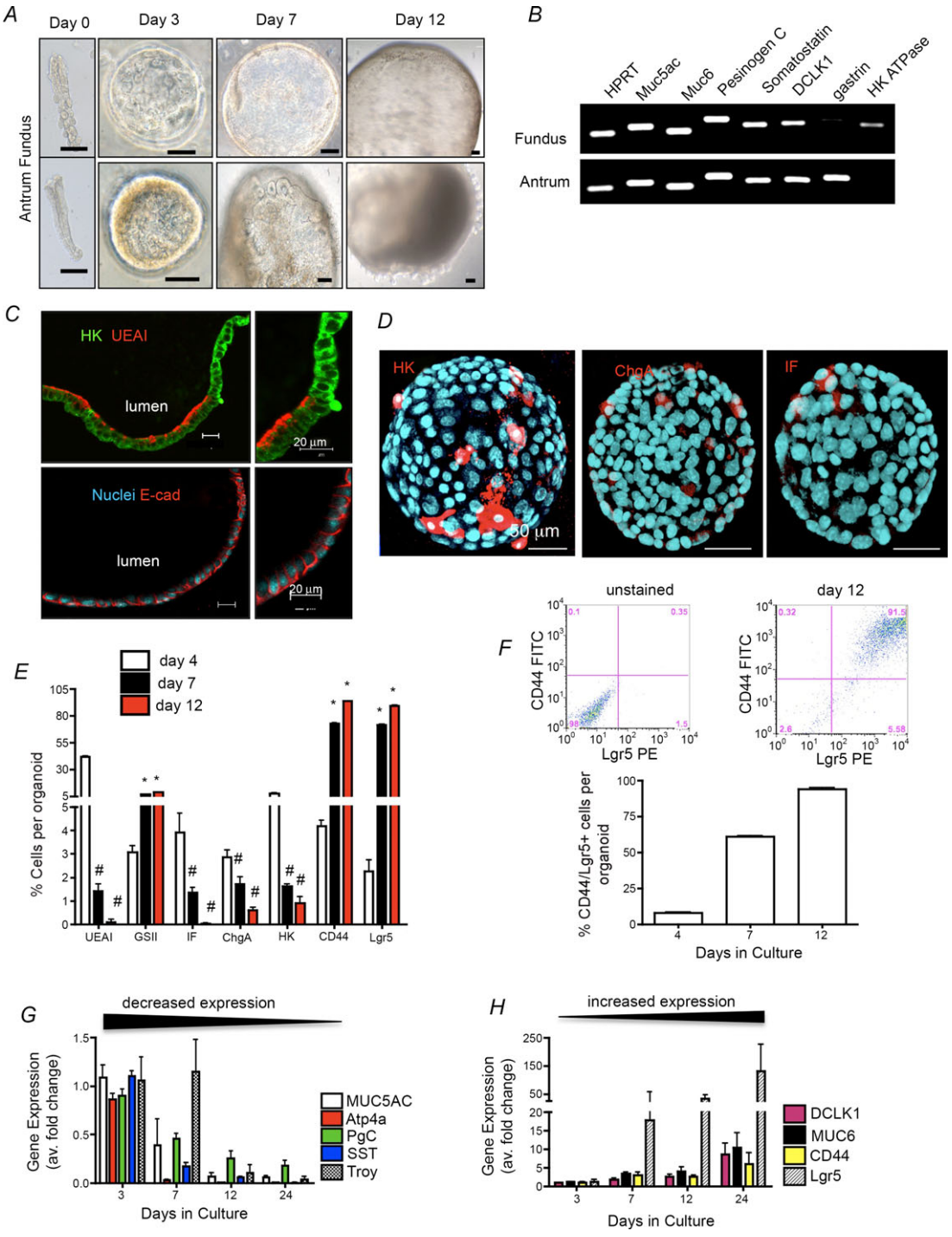

Figure 4. Model 1: fundic gastric organoids used in the expansion of stem/progenitor cells
A, cyst-like 3D structures grown from fundic or antral gastric glands isolated from mouse. Images from 0, 3, 7 and 12 day cultures. Scale bars = 50 μm. *B*, RT-PCR analysis of gastric lineage markers at culture day 12. Both fundic and antral organoids expressed mRNA for mucin 5AC (surface mucous pit cells), mucin 6 (mucous neck cells), pepsinogen C (zymogen/chief cells) and somatostatin (D cells). In contrast, the expression of gastrin (G cells) was specific to antral organoids whereas H^+,K^+-ATPase (parietal cells) was specific to fundic organoids. *C*, organoid sections immunostained for H^+,K^+-ATPase (HK, green) and UEAI (red), and E-cadherin (red) and Hoechst (nuclear, blue) Scale bars = 20 μm. *D*, organoids immunostained for HK (red), chromogranin A (chgA, red), intrinsic factor (IF, red) and Hoechst (nuclear, blue). Scale bars = 50 μm. *E*, flow cytometric analysis using fundic organoids at 4, 7 and 12 days in culture. *F*, 2D flow cytometric histogram of gated cells co-expressing CD44 and Lgr5. *G* and *H*, qRT-PCR of cell lineage and gastric stem cell markers using RNA isolated from organoids cultured for 3, 7 and 12 days. $^{\#}P < 0.05$ compared with day 4, $n = 4$ individual organoid preparations.

model 1 (Fig. 6*E*, *F*). Proliferation was restored in model 1 after passage (data not shown). Cells within the model 1 culture system increased in proliferation after passage (data not shown). Such data suggest that the gastric organoids in model 1 cannot be maintained in culture indefinitely without passage.

Markers of intestinal metaplasia and SPEM are expressed in cultured fundic gastric organoids

The one differentiated marker that increased in model 1 was GSII (Fig. 4*E*). Given that this marker has also been implicated in the development of metaplasia, in particular spasmolytic polypeptide expressing metaplasia (SPEM) (Nozaki *et al.* 2008), other metaplastic markers were measured by qRT-PCR in models 1 and 2 using 4, 7 and 12 day cultures (Fig. 7). When compared with the expression levels in native tissue, expression of markers of intestinal metaplasia that included Cdx1 (Fig. 7*A*), MUC2 (Fig. 7*C*) and TFF3 (Fig. 7*D*) significantly decreased in both models with culture. However, compared with the native tissue, Cdx2 expression was significantly upregulated in day 4 cultures of models 1 and 2 (Fig. 7*B*). Expression of Cdx2 significantly decreased in both models over 12 days in culture (Fig. 7*B*). HE4, typically elevated during metaplasia (Nozaki *et al.* 2008), significantly increased in the organoid cultures relative to expression in the native tissue (Fig. 7*E*). While TFF2 was significantly increased in model 1 over 12 days in culture, expression of TFF2 significantly decreased in model 2 over time (Fig. 7*F*). Collectively, these data show that Cdx2, a marker of intestinal metaplasia (Moskaluk *et al.* 2003), was upregulated during the initial culture of the gastric organoids. In addition, SPEM marker HE4 was also increased in the gastric organoids compared with expression levels in native tissue.

Fundic gastric organoids consist of functional parietal cells

To assess parietal cell function, a pH-sensitive dye was injected into the lumen of organoids with or without ISMC co-culture. Histamine induced a significant decrease in intraluminal pH that was reversed by omeprazole in fundic organoids (*Fig.* 8*A*, *B*). Notably, the response to histamine and omeprazole was greater in co-cultured organoids (Fig. 8*B*). Antrum-derived cultures appeared to respond to histamine but not to omeprazole treatment (Fig. 8*C*, *D*). The changes in pH observed in the antrum-derived organoids may be attributed to metabolic changes. Moreover, the lack of response to omeprazole within the antrally derived cultures suggests that the response to histamine was not attributed to parietal cell function. Thus, fundic gastric organoids were also found to maintain a functional epithelium. These data demonstrate a primary culture system of healthy fundic gastric organoids that retain differentiated epithelial characteristics.

Transmission electron microscopy revealed a secretory membrane in parietal cells within the organoids. The parietal cells within the organoids exhibited well-developed canaliculi that appeared to be well organized within the cell with long microvilli (Fig. 9*A*, *B*). Therefore, we further investigated whether the parietal cells in the fundic organoids are capable of acid secretion in response to histamine. Acridine Orange, a fluorescence dye, is known to show green fluorescence (maximum excitation: 503 nm, emission: 526 nm) at a neutral pH, whereas its fluorescent spectrum shifts to red (maximum excitation: 460 nm, emission: 650 nm) when it accumulates in the acidic organelles, such as the secretory canaliculus of parietal cells (Lambrecht *et al.* 2005). In response to histamine, Acridine Orange accumulated in cell vesicles as indicated in Fig. 9*C* (cells identified by white circles 1–5), which was accompanied by an increase in the ratio of F458 (red)/F488 (green) (Fig. 9*D*). These results indicated the generation of protons present within the secretory canaliculi. No accumulation was observed before histamine treatment. Collectively, these results indicate that functional parietal cells exist in the fundic organoids.

Fundic gastric organoids used to study epithelial restitution

We used an established photodamage model of cell damage (Nyqvist *et al.* 2005; Xue *et al.* 2011; Aihara *et al.* 2013) to test the use of fundic organoid culture in studies of cell migration/repair. Localized photodamage (Fig. 10*A*, red rectangle) resulted in the loss of YFP and rapid dead cell exfoliation (Fig. 10*A*, arrow 2) coincident with migration of neighbouring cells to the damaged area (Fig. 10*A*, arrow 3), sustaining epithelial continuity (Fig. 10*A*, arrow 4), similar to what is seen *in vivo* (Nyqvist *et al.* 2005; Xue *et al.* 2011; Aihara *et al.* 2013) (Video S3). Damaged cells were exfoliated into the lumen following photodamage, while Lucifer yellow did not leak into the lumen, suggesting that the integrity of the epithelium was maintained (Fig. 10*B*).

Discussion

The fundic organoid culture model represents a significant advance in our ability to replicate the gastrointestinal environment *in vitro*. We concluded from these studies that: (1) with extended culture, fundic gastric organoids are an ideal model for the enrichment of a stem cell-like niche, (2) with ISMC co-culture an epithelium expressing mature cell lineages can be maintained *in vitro* and (3) fundic gastric organoids can be used for the study of gastric physiology and disease (Fig. 1). Major efforts were

made to produce the gastric organoids specifically from the fundic region of the stomach because of the advantages this model has over existing models. For example, the simple AGS gastric cancer cell line is a useful tool for studying *Helicobacter pylori* adherence and pathogenesis (Zhang *et al.* 2002). However, despite extensive evidence demonstrating that *H. pylori* induces gastric epithelial changes, the direct impact of the bacterium on the normal gastric epithelium independent of systemic factors has never been studied. The gastric organoids make it possible for us to study the direct interaction between the bacteria and the normal gastric epithelium (Schumacher *et al.* 2014). Furthermore, gastric acid secretion can be measured in isolated gastric glands (Lambrecht *et al.* 2005), but unlike the organoid culture system, gastric glands cannot be maintained indefinitely *in vitro* making

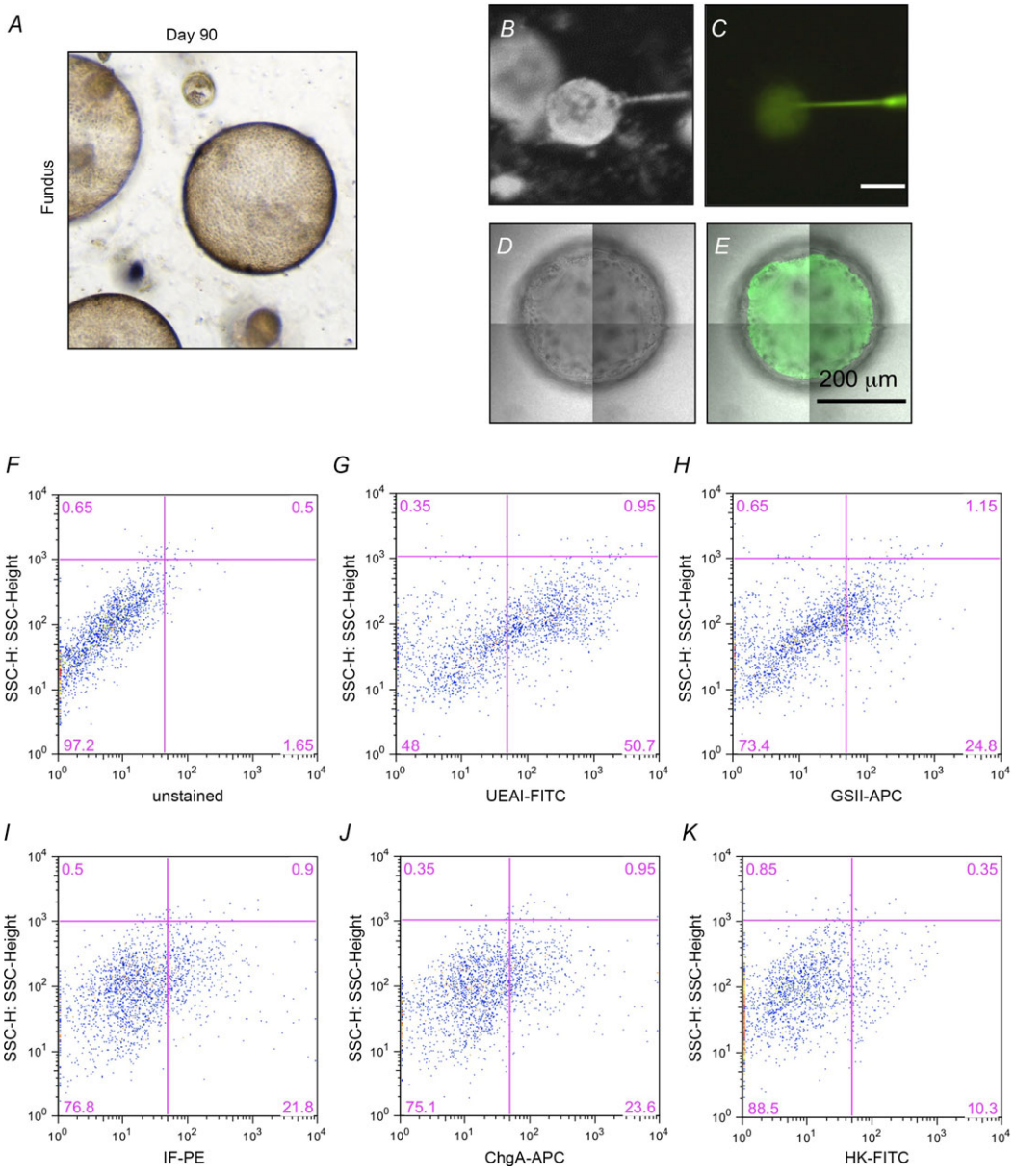

Figure 5. Transepithelial permeability and flow cytometric analysis of fundic organoids
A, fundic gastric organoid maintained in culture for 90 days. *B–E*, injection and retention of Lucifer yellow (LY) within the organoid lumen after injection. Luminal retention of microinjected Lucifer yellow over 24 h confirmed low transepithelial permeability of fundic organoids. Stereoscopic images of organoids during LY injection in bright-field (*B*) or fluorescence (*C*), and confocal images of organoids 1 day after LY injection in bright-field (*D*) or fluorescence plus bright-field (*E*). *F–K*, representative flow cytometric dot plots showing the gating scheme and cell distribution of UEAI (surface pit), GSII (mucous neck), IF (intrinsic factor, chief), ChgA (endocrine) and HK (H^+,K^+-ATPase, parietal) cells in gastric organoids.

long-term studies difficult. Thus, overall cultured stem cells into gastric organoids certainly have advantages over these simpler *in vitro* systems.

Cellular quantification for the major gastric cell lineage markers demonstrated that with extended culture we enriched for a stem cell-like niche. By day 12 and following passage of organoids, there was a decrease in the relative expression of mature cells within the organoid. However, reported markers for putative gastric stem cells such as Lgr5 (Barker *et al.* 2010) and CD44 (Khurana *et al.* 2013) were increased. The hyaluronic receptor CD44 (Aruffo *et al.* 1990) has been identified as a potential gastric stem cell marker of the fundus. Notably, CD44-positive undifferentiated cells have been located within the isthmus region of the fundus, precisely where the stem cells are known to reside (Khurana *et al.* 2013). Unpublished data from our laboratory also show that single CD44-positive cells isolated from the fundus give rise to organoids in

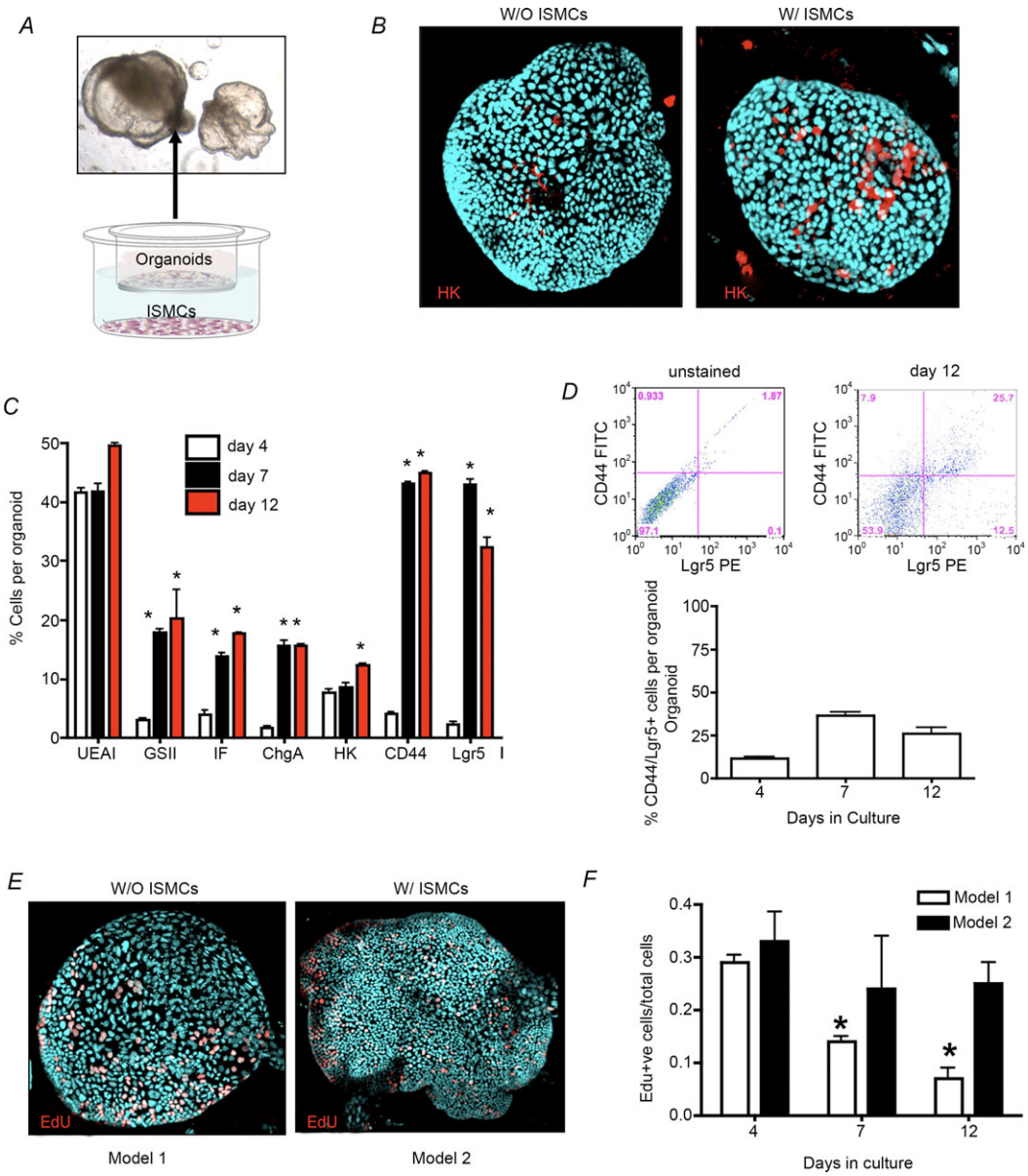

Figure 6. Model 2: Maintenance of epithelial cells within fundic gastric organoids co-cultured with ISMCs
A, organoid/ISMC co-culture Transwell system showing morphological changes in organoids. *B*, organoids in whole mount immunostained for H^+,K^+-ATPase (HK, red), and Hoechst (nuclear, blue) co-cultured without (W/O) or with (W/) ISMCs. *C*, flow cytometric analysis using fundic organoids co-cultured with ISMCs for 4, 7 and 12 days in culture. *D*, 2D flow cytometric histogram of gated cells co-expressing CD44 and Lgr5. *E* and *F*, EdU immunostaining (EdU: red, nuclear: blue) (*E*) followed by quantification of Edu+ nuclei/total cell number (*F*).

culture. Thus, CD44-positive cells have the capacity to undergo cell division that may give rise to differentiated gastric epithelial cells. The increase in Lgr5 was surprising given that this stem cell marker is expressed in the fundus during development alone (Barker *et al.* 2010), and suggests a reversion from a mature to an immature phenotype when using the specified gastric organoid growth culture conditions.

While cells expressing stem cell markers CD44 and Lgr5 expanded with passage, *Troy* expression declined. It is

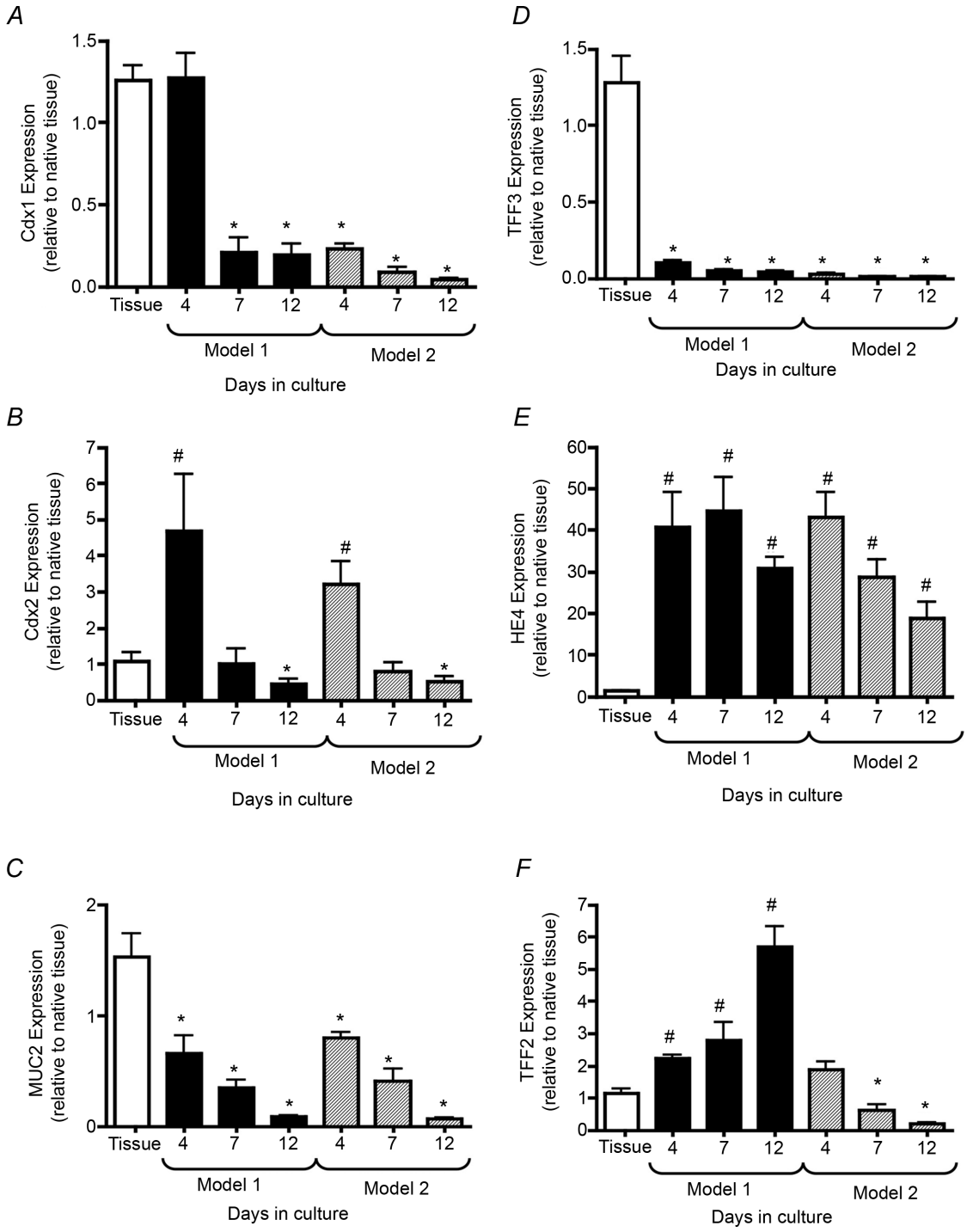

Figure 7. Expression of metaplastic markers in cultures of gastric organoids of model 1 and model 2
qRT-PCR of metaplastic markers Cdx1 (*A*), Cdx2 (*B*), MUC2 (*C*), TFF3 (*D*), HE4 (*E*) and TFF2 (*F*) using RNA isolated from organoids cultured for 4, 7 and 12 days. $^{*}P < 0.05$, significantly decreased compared with native tissue; $^{\#}P < 0.05$, significantly increased compared with native tissue; $n = 3$ individual organoid preparations.

accepted that stem cells anchored in the isthmus region are responsible for the production of parietal cells (Karam & Leblond, 1993), and appear to be distinct from the recently identified stem cells marked by *Troy* (Stange *et al.* 2013). *Troy*-positive cells are expressed at the corpus gland base in a subset of differentiated chief cells (Stange *et al.* 2013). Stange *et al.* (2013) demonstrate that *Troy*-positive chief cells may be used to generate long-lived gastric organoids, and *in vitro* these cultures are differentiated toward the mucus-producing cell lineages of the neck and pit regions. The *Troy*-derived organoids are distinct from the cultures that are derived from whole dissociated glands reported here such that we have devised a method to maintain all the major cell lineages of the fundus.

To maintain a mature phenotype we implemented a Transwell system whereby gastric organoids were co-cultured with ISMCs (Shaulian *et al.* 1992; Feng *et al.* 2014). We observed a significant induction in the expression of the major cell lineages when compared with the expression levels of 12-day-old organoid cultures. The ISMCs are shown to induce embryonic endoderm to differentiate to a gastric phenotype (Kim *et al.* 2005). An interesting study by Kim *et al.* (2005) demonstrated that by epithelial–mesenchymal co-cultures homeobox gene Barx1 (normally confined to the stomach mesenchyme) drives stomach epithelial differentiation via the inhibition of Wnt signalling. Therefore, we may speculate that in the current co-culture system Barx1 may play a similar role in the differentiation of the gastric organoids, but this requires further investigation.

Cdx2, a marker of intestinal metaplasia (Moskaluk *et al.* 2003), was upregulated during the initial culture of the gastric organoids. These data suggest that initially the cultures are metaplastic and with time in culture cells revert back to normal differentiation. SPEM marker HE4 was also increased in the gastric organoids when compared

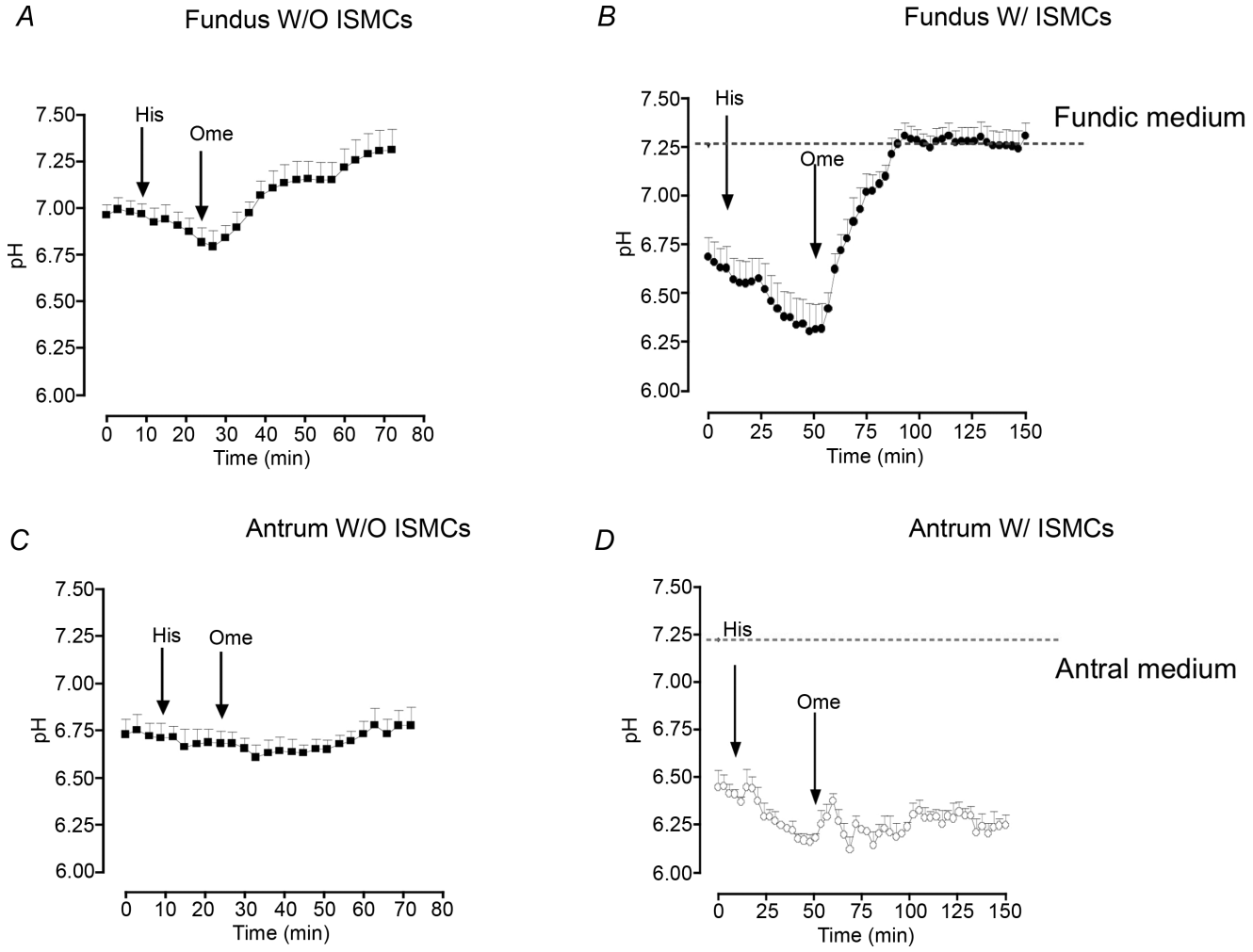

Figure 8. Organoid-derived parietal cell functional assay
Intraluminal pH response to histamine (His) and omeprazole (Ome) using fundic organoids cultured without (W/O) ISMCs (*A*) or with (W/) ISMCs (*B*). Intraluminal pH response to His and Ome using antral organoids cultured W/O ISMCs (*C*) or W/ ISMCs (*D*). $n = 6$ individual organoids.

with expression levels in native tissue. HE4 has been shown to be up-regulated in gastric metaplasia in both mice and humans and its expression is maintained in gastric adenocarcinomas (Nozaki *et al.* 2008). Although HE4 was upregulated initially in the gastric organoids, expression significantly decreased with culture time in model 2. Interestingly, it has been suggested that SPEM cells re-differentiate to chief cells in the process of tissue repair such as that observed during ulcer healing (Kikuchi *et al.* 2010). Perhaps HE4 is up-regulated in the organoids as a mechanism of cellular proliferation and repair during the development of the spheres. Notably, TFF2 significantly increased over time in model 1. Consistent with the enrichment of stem cells in model 1 of our gastric organoid cultures, TFF2 transcript-expressing cells have been shown to be progenitors for mucus neck, parietal and zymogenic cells in the oxyntic gastric mucosa (Quante *et al.* 2010).

Fundic gastric organoids were also found to maintain a functional epithelium. Histamine induced a significant

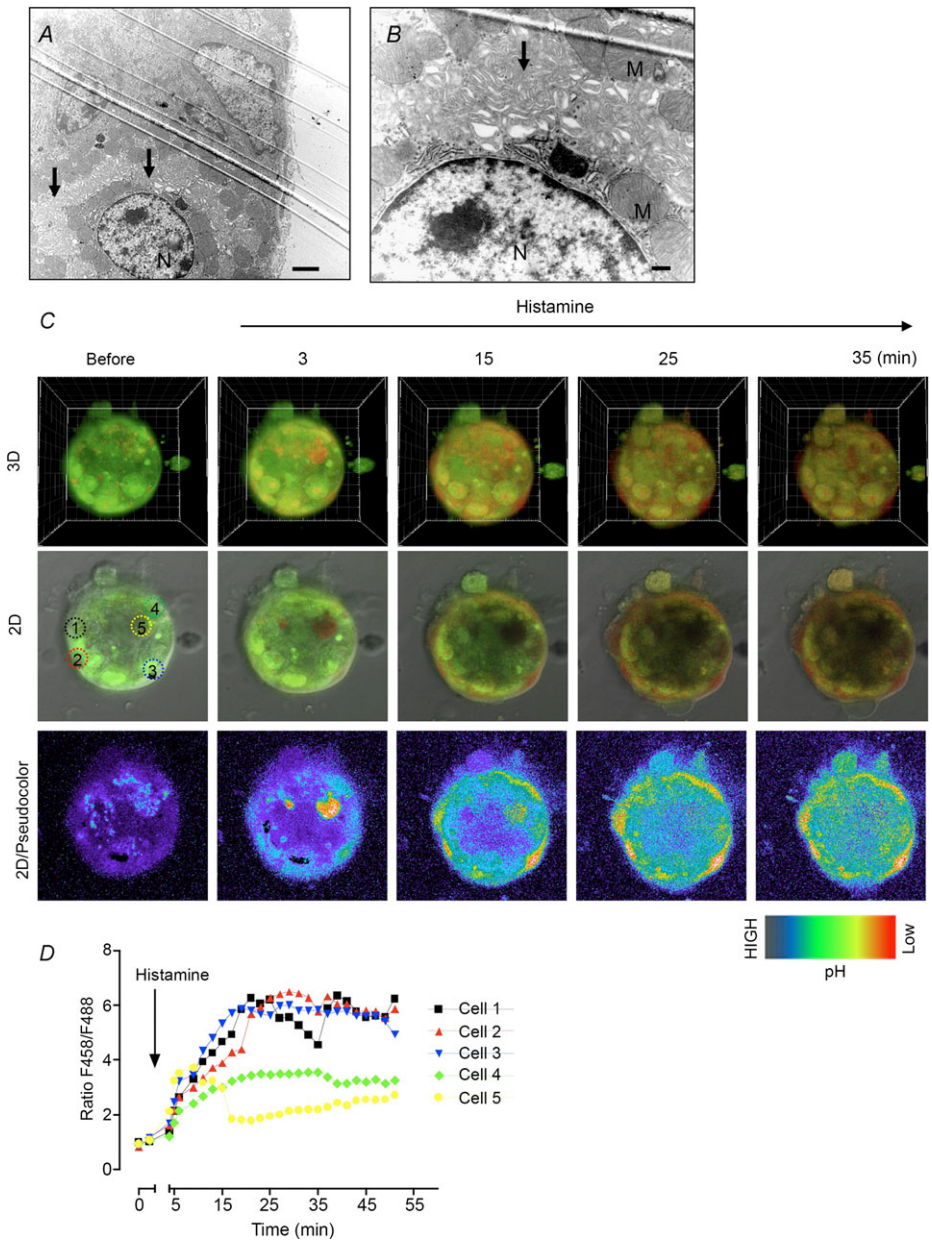

Figure 9. Presence of parietal cells in the fundic gastric organoids
A and *B*, observation of parietal cells within the fundic organoid at low (*A*) or high (*B*) magnification by transmission electron microscopy. N, nuclear; M, mitochondria. *C*, confocal images of a fundic organoid labelled with Acridine Orange before and after histamine (100 μM). Images shows 3D, 2D or pseudocolour of F458 (red)/F488 (green), respectively. *D*, changes in the ratio F458/F488 in response to histamine from five individual cells indicated in *C*.

decrease in intraluminal pH that was reversed by omeprazole in fundic organoids. These observations supported numerous physiological studies showing that histamine released from the enterochromaffin-like (ECL) cells stimulates acid secretion from parietal cells within the gastric epithelium (Prinz *et al.* 1993; Waldum *et al.* 1996). Omeprazole blocks histamine-induced acid secretion by specifically binding to the H^+,K^+-ATPase on the parietal cells (Wallmark *et al.* 1983). Notably, the response to histamine was greater in co-cultured organoids and correlated with the presence of greater numbers of parietal cells within the epithelium. In contrast to the fundic organoids, while antrum-derived cultures respond to histamine these cultures do not respond to omeprazole. The changes in pH observed in the antrally derived organoids may be attributed to metabolic changes. The lack of response to omeprazole within the antrally derived cultures suggests that the response to histamine was not attributed to parietal cell function. Overall, there was a minor pH difference with surrounding media compared with the *in vivo* pH of the stomach. This high pH *in vitro* is attributed to the buffering of the surrounding media and also the significantly lower number of parietal cells within organoids compared with native tissue. In addition, we demonstrated that the fundic organoid culture may be used in studies of cell migration/repair. Localized photodamage consistently resulted in rapid dead cell exfoliation into the lumen, similar to what is seen *in vivo* (Nyqvist *et al.* 2005; Xue *et al.* 2011; Aihara *et al.* 2013). Moreover, neighbouring cells formed lamellipodia and migrated toward and sealed the damaged area, suggesting that gastric organoids may also be used for the study of cell migration. These data demonstrate a primary culture system of healthy fundic gastric organoids that

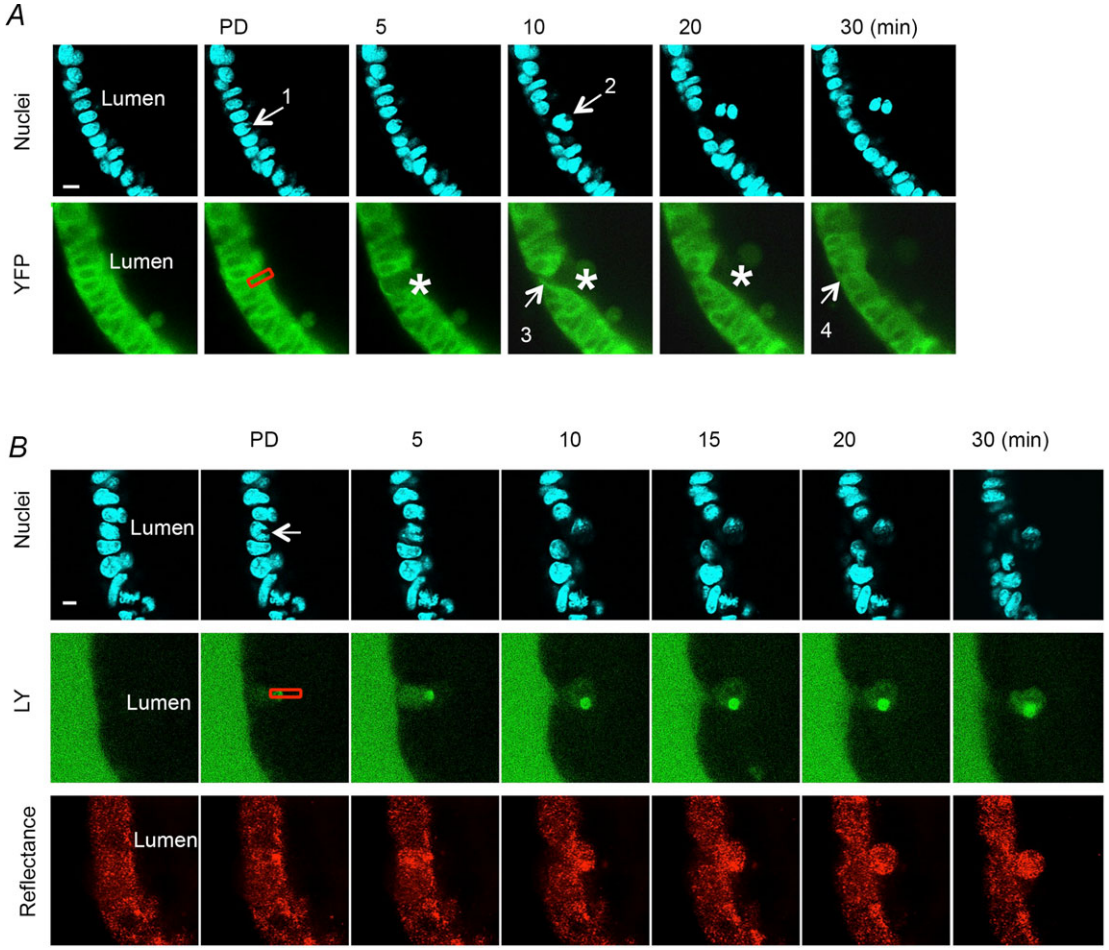

Figure 10. Fundic gastric organoids used to study epithelial restitution
A, two-photon damage (at site indicated by arrow 1 and red box) results in cell exfoliation into the lumen and restoration of the damaged epithelium within 30 min. Blue = nuclear stain; green = endogenous YFP cytoplasmic fluorescence of fundic organoids from YC transgenic mouse cells. *B*, maintenance of epithelial barrier following cell damage. Two-photon damage (at site indicated by arrow 1 and red box) results in cell exfoliation into the lumen and restoration of the damaged epithelium within 30 min. The entrance of Lucifer yellow-containing extraluminal medium into the lumen of the organoid is limited. Blue = nuclear stain; green = Lucifer yellow; Red = reflectance.

retain differentiated epithelial characteristics and mimic the native tissue responses.

Although the organoid culture system has been extensively used for the study of stem cell biology and gastrointestinal development (Jaks *et al.* 2008; Barker *et al.* 2010; Stange *et al.* 2013), here we report for the first time the degree to which these cultures reflect the function of native tissue. Moreover, we detail the cellular nature of two fundic gastric organoid culture models and the capacity for use in functional studies of physiological research. We have developed two gastric fundically derived organoid spheroid cultures. Model 1 can be used for the expansion of gastric fundic stem cells for studies that may include stem cell biology and tissue repair/regeneration (Fig. 1). Model 2 can be used for studies of physiological function/gastric disease and epithelial cell biology whereby the maintenance of mature cell lineages is required (Fig. 1). These results suggest that gastric fundic organoids have utility in studies of epithelial cell biology, cell damage and bacterial–epithelial interactions.

A limitation of the fundic organoid system, as for other reported gastric organoids (Barker *et al.* 2010; Stange *et al.* 2013; Bartfeld *et al.* 2015), is that these systems do not recapitulate the native tissue exactly. As demonstrated in the current study, although the cellular composition, polarity and response to acid secretagogues are similar to the native tissue, the gland architecture and cell arrangement are lost in the organoids. However, unlike gastric cancer cell lines that have been typically used for the study of *H. pylori* pathogenesis, the fundic organoid culture represents a significant advance in our ability to replicate the gastrointestinal environment *in vitro*. Alternatively, a recent study reports the generation of 3D human gastric tissue *in vitro* through the directed differentiation of human pluripotent stem cells (McCracken *et al.* 2014). The antral gastric organoids derived from human pluripotent stem cells exhibit the geographical distribution of cell lineages similar to that observed in the native tissue (McCracken *et al.* 2014) and may be used as a complimentary model in comparison to the fundic gastric organoids.

In the past, the small intestinal submucosa was used as a scaffold for gastrointestinal restoration because of its acellular biodegradable collagen-rich matrix containing functional growth factors, such as basic fibroblast growth factor (bFGF), vascular endothelial growth factor (VEGF) and transforming growth factor-β (TGFβ), which are considered vital to the regenerative process (Voytik-Harbin *et al.* 1997; McDevitt *et al.* 2003; Hodde *et al.* 2007). The small intestinal submucosa has been commonly used as a bioscaffold for the replacement of various gastrointestinal tracts in animals, including the oesophagus (Doede *et al.* 2009), small intestine (Chen & Badylak, 2001; Wang *et al.* 2003; Lee *et al.* 2008; Qin & Dunn, 2011), colon (Ueno *et al.* 2007*b*; Hoeppner *et al.* 2009) and stomach (de la Fuente *et al.* 2003; Ueno *et al.* 2007*a*; Nishimura *et al.* 2010; Nakatsu *et al.* 2013). Alternatively, adult stem cell therapy using gastrointestinal organoids may hold promise for the treatment of gastrointestinal diseases. The feasibility of colon stem cell therapy based on the simple *in vitro* expansion of a single adult colonic stem cell has been reported (Yui *et al.* 2012). However, whether gastrically derived organoids may be used for stomach regeneration and the treatment of disease remains to be investigated.

References

Aihara E, Hentz CL, Korman AM, Perry NP, Prasad V, Shull GE & Montrose MH (2013). *In vivo* epithelial wound repair requires mobilization of endogenous intracellular and extracellular calcium. *J Biol Chem* **288**, 33585–33597.

Aruffo A, Stamenkovic I, Melnick M, Underhill CB & Seed B (1990). CD44 is the principal cell surface receptor for hyaluronate. *Cell* **61**, 1303–1313.

Barker N, Huch M, Kujala P, vande Wetering M, Snippert H, vanEs JH, Sato T, Stange DE, Begthel H, vanden Born M, Danenberg E, vanden Brink S, Korving J, Abo A, Peters PJ, Wright N, Poulsom R & Clevers H (2010). Lgr5(+ve) stem cells drive self-renewal in the stomach and build long-lived gastric units *in vitro*. *Cell Stem Cell* **6**, 25–36.

Bartfeld S, Bayram T, vande Wetering M, Huch M, Begthel H, Kujala P, Vries R, Peters PJ & Clevers H (2015). *In vitro* expansion of human gastric epithelial stem cells and their responses to bacterial infection. *Gastroenterology* **148**, 126–136.

Bell SM, Schreiner CM, Wert SE, Mucenski ML, Scott WJ & Whitsett JA (2008). R spondin 2 is required for normal laryngeal–tracheal, lung and limb morphogenesis. *Development* **135**, 1049–1058.

Chen MK & Badylak SF (2001). Small bowel tissue engineering using small intestinal submucosa as a scaffold. *J Surg Res* **99**, 352–358.

Chu S & Montrose MH (1995). Extracellular pH regulation in microdomains of colonic crypts: effects of short-chain fatty acids. *Proc Natl Acad Sci U S A* **92**, 3303–3307.

dela Fuente SG, Gottfried MR, Lawson DC, Harris MB, Mantyh CR & Pappas TN (2003). Evaluation of porcine-derived small intestine submucosa as a biodegradable graft for gastrointestinal healing. *J Gastrointest Surg* **7**, 96–101.

Doede T, Bondartschuk M, Joerck C, Schulze E & Goernig M (2009). Unsuccessful alloplastic esophageal replacement with porcine small intestinal submucosa. *Artif Organs* **33**, 328–333.

Feng R, Aihara E, Kenny S, Yang L, Li J, Varro A, Montrose MH, Shroyer NF, Wang TC, Shivdasani RA & Zavros Y (2014). Indian Hedgehog mediates gastrin-induced proliferation in stomach of adult mice. *Gastroenterology* **147**, 655–666.

Hodde J, Janis A, Ernst D, Zopf D, Sherman D & Johnson C (2007). Effects of sterilization on an extracellular matrix scaffold: part I. Composition and matrix architecture. *J Mater Sci Mater Med* **18**, 537–543.

Hoeppner J, Crnogorac V, Marjanovic G, Jüttner E, Keck T, Weiser HF & Hopt UT (2009). Small intestinal submucosa for reinforcement of colonic anastomosis. *Int J Colorectal Dis* **24**, 543–550.

Jaks V, Barker N, Kasper M, vanEs JH, Snippert HJ, Clevers H & Toftgård R (2008). Lgr5 marks cycling, yet long-lived, hair follicle stem cells. *Nat Genet* **40**, 1291–1299.

Karam SM & Leblond CP (1993). Dynamics of epithelial cells in the corpus of the mouse stomach. I. Identification of proliferative cell types and pinpointing of the stem cell. *Anat Rec* **236**, 259–279.

Khurana SS, Riehl TE, Moore BD, Fassan M, Rugge M, Romero-Gallo J, Noto J, Peek RMJ, Stenson WF & Mills JC (2013). The hyaluronic acid receptor CD44 coordinates normal and metaplastic gastric epithelial progenitor cell proliferation. *J Biol Chem* **288**, 16085–16097.

Kikuchi M, Nagata H, Watanabe N, Watanabe H, Tatemichi M & Hibi T (2010). Altered expression of a putative progenitor cell marker DCAMKL1 in the rat gastric mucosa in regeneration, metaplasia and dysplasia. *BMC Gastroenterol* **10**, 65.

Kim BM, Buchner G, Miletich I, Sharpe PT & Shivdasani RA (2005). The stomach mesenchymal transcription factor Barx1 specifies gastric epithelial identity through inhibition of transient Wnt signaling. *Dev Cell* **8**, 611–622.

Lambrecht NW, Yakubov I, Scott D & Sachs G (2005). Identification of the K efflux channel coupled to the gastric H–K-ATPase during acid secretion. *Physiol Genomics* **21**, 81–91.

Lee M, Chang PC & Dunn JC (2008). Evaluation of small intestinal submucosa as scaffolds for intestinal tissue engineering. *J Surg Res* **147**, 168–171.

Livak KJ & Schmittgen TD (2001). Analysis of relative gene expression data using real-time quantitative PCR and the $2^{-\Delta\Delta CT}$ method. *Methods* **25**, 402–408.

McCracken KW, Catá EM, Crawford CM, Sinagoga KL, Schumacher M, Rockich BE, Tsai YH, Mayhew CN, Spence JR, Zavros Y & Wells JM (2014). Modelling human development and disease in pluripotent stem-cell-derived gastric organoids. *Nature* **516**, 400–404.

McDevitt CA, Wildey GM & Cutrone RM (2003). Transforming growth factor-β1 in a sterilized tissue derived from the pig small intestine submucosa. *J Biomed Mater Res A* **67**, 637–640.

Mills JC & Shivdasani RA (2011). Gastric epithelial stem cells. *Gastroenterology* **140**, 412–424.

Moskaluk CA, Zhang H, Powell SM, Cerilli LA, Hampton GM & Frierson HFJ (2003). Cdx2 protein expression in normal and malignant human tissues: an immunohistochemical survey using tissue microarrays. *Mod Pathol* **16**, 913–919.

Nakatsu H, Ueno T, Oga A, Nakao M, Nishimura T, Kobayashi S & Oka M (2013). Influence of mesenchymal stem cells on stomach tissue engineering using small intestinal submucosa. *J Tissue Eng Regen Med* doi: 10.1002/term.1794.

Nishimura T, Ueno T, Nakatsu H, Oga A, Kobayashi S & Oka M (2010). *In vivo* motility evaluation of the grafted gastric wall with small intestinal submucosa. *Tissue Eng Part A* **16**, 1761–1768.

Nozaki K, Ogama M, Williams JA, Lafleur BJ, Ng V, Drapkin RI, Mills JC, Konieczny SF, Nomura S, Goldenring JR (2008). A molecular signature of gastric metaplasia arising in response to acute parietal cell loss. *Gastroenterology* **134**, 511–522.

Nyqvist D, Mattsson G, Köhler M, Lev-Ram V, Andersson A, Carlsson PO, Nordin A, Berggren PO & Jansson L (2005). Pancreatic islet function in a transgenic mouse expressing fluorescent protein. *J Endocrinol* **186**, 333–341.

Prinz C, Kajimura M, Scott DR, Mercier F, Helander HF & Sachs G (1993). Histamine secretion from rat enterochromaffinlike cells. *Gastroenterology* **105**, 449–461.

Qin HH & Dunn JC (2011). Small intestinal submucosa seeded with intestinal smooth muscle cells in a rodent jejunal interposition model. *J Surg Res* **171**, 21–26.

Quante M, Marrache F, Goldenring JR & Wang TC (2010). TFF2 mRNA transcript expression marks a gland progenitor cell of the gastric oxyntic mucosa. *Gastroenterology* **139**, 2018–2027.

Schumacher MA, Feng R, Aihara E, Engevik AC, Montrose MH, Ottemann KM & Zavros Y (2014). *Helicobacter pylori*-induced Sonic Hedgehog expression is regulated by NFκB pathway activation: the use of a novel in vitro model to study epithelial response to infection. *Helicobacter* **20**, 19–28.

Shaulian E, Zauberman A, Ginsberg D & Oren M (1992). Identification of a minimal transforming domain of p53: negative dominance through abrogation of sequence-specific DNA binding. *Mol Cell Biol* **12**, 5581–5592.

Stange DE, Koo BK, Huch M, Sibbel G, Basak O, Lyubimova A, Kujala P, Bartfeld S, Koster J, Geahlen JH, Peters PJ, vanEs JH, vande Wetering M, Mills JC & Clevers H (2013). Differentiated Troy$^+$ chief cells act as reserve stem cells to generate all lineages of the stomach epithelium. *Cell* **155**, 357–368.

Ueno T, dela Fuente SG, Abdel-Wahab OI, Takahashi T, Gottfried M, Harris MB, Tatewaki M, Uemura K, Lawson DC, Mantyh CR & Pappas TN (2007*a*). Functional evaluation of the grafted wall with porcine-derived small intestinal submucosa (SIS) to a stomach defect in rats. *Surgery* **142**, 376–383.

Ueno T, Oga A, Takahashi T & Pappas TN (2007*b*). Small intestinal submucosa (SIS) in the repair of a cecal wound in unprepared bowel in rats. *J Gastrointest Surg* **11**, 918–922.

Voytik-Harbin SL, Brightman AO, Kraine MR, Waisner B & Badylak SF (1997). Identification of extractable growth factors from small intestinal submucosa. *J Cell Biochem* **67**, 478–491.

Waldum HL, Arnestad JS, Brenna E, Eide I, Syversen U & Sandvik AK (1996). Marked increase in gastric acid secretory capacity after omeprazole treatment. *Gut* **39**, 649–653.

Wallmark B, Sachs G, Mardh S & Fellenius E (1983). Inhibition of gastric ($H^+ + K^+$)-ATPase by the substituted benzimidazole, picoprazole. *Biochim Biophys Acta* **728**, 31–38.

Wang ZQ, Watanabe Y & Toki A (2003). Experimental assessment of small intestinal submucosa as a small bowel graft in a rat model. *J Pediatr Surg* **38**, 1596–1601.

Xue L, Aihara E, Wang TC & Montrose MH (2011). Trefoil factor 2 requires Na/H exchanger 2 activity to enhance mouse gastric epithelial repair. *J Biol Chem* **286**, 38375–38382.

Yui S, Nakamura T, Sato T, Nemoto Y, Mizutani T, Zheng X, Ichinose S, Nagaishi T, Okamoto R, Tsuchiya K, Clevers H & Watanabe M (2012). Functional engraftment of colon epithelium expanded *in vitro* from a single adult $Lgr5^+$ stem cell. *Nat Med* **18**, 618–623.

Zhang ZW, Dorrell N, Wren BW & Farthingt MJ (2002). *Helicobacter pylori* adherence to gastric epithelial cells: a role for non-adhesin virulence genes. *J Med Microbiol* **51**, 495–502.

Additional information

Conflict of interest

None declared.

Author contributions

M.A.S., E.A., R.F., A.E., N.F.S., K.M.O., R.T.W., M.H.M., R.A.S. and Y.Z. conceived and designed the experiments; drafted the article or revised it critically for important intellectual content. M.A.S., E.A., R.F., A.E. and Y.Z. collected, analysed and interpreted the data.

Funding

This work was supported by the American Gastroenterological Association: Robert and Sally Funderburg Research Award in Gastric Cancer and R01 DK083402 grant (Y.Z.), the Albert J. Ryan Fellowship (M.A.S.) and R01 DK54940 (M.H.M.). This project was supported in part by PHS Grant P30 DK078392 (Integrative Morphology Core) and NIH AR-47363 (Research Flow Cytometry Core in the Division of Rheumatology) of the Digestive Diseases Research Core Centre in Cincinnati.

Acknowledgements

We gratefully acknowledge Drs Meritxell Huch, Sina Bartfeld and Hans Clevers (Hubrecht Institute for Developmental Biology and Stem Cell Research, Netherlands) for the kind gift of L cells and for technical discussions. We also acknowledge Dr Jeffrey Whitsett (Section of Neonatology, Perinatal and Pulmonary Biology, Cincinnati Children's Hospital Medical Centre and The University of Cincinnati College of Medicine, Cincinnati, OH)for kindly donating the modified HEK-293T cells. We thank Lisa MacMillan (Pathology Research Core, Cincinnati Children's Hospital Medical Centre) for embedding and tissue processing.

Supporting information

The following supporting information is available in the online version of this article.

Video S1. Growth of fundus-derived organoid.
Video S2. Growth of antrum-derived organoid.
Video S3. Two-photon-induced damage (photodamage, PD) at fundic organoid apical side repairs rapidly with cell exfoliation to lumen. Red = reflectance, blue = nuclei, green = YFP, and merged. PD created at 30 s at cell indicated by arrow.